

# Experiments with Transparent Teleoperation under Position and Rate Control

Wen-Hong Zhu

S. E. Salcudean

Ming Zhu

Dept. of Electrical and Computer Engineering  
University of British Columbia  
2356 Main Mall, Vancouver, BC  
Canada V6T 1Z4

## Abstract

*A four-channel data transmission structure has been proposed in the literature to achieve "transparency" for master-slave teleoperator systems under both position and rate control [1]. In this paper, experimental results for a one degree-of-freedom system are given to demonstrate that the proposed scheme possesses good stability and transparency under both position and rate control in contact with both flexible and rigid environments. A unilateral constraint correction under rate control is also discussed.*

## 1 Introduction

From its early use in the remote manipulation of radioactive materials, the meaning of teleoperation has expanded to include manipulation at a different scale and in virtual worlds [2, 3, 4]. Teleoperation systems have the potential to play an important role in space and undersea exploration and servicing, forestry and mining, microsurgery and microassembly.

Contact information is helpful to the operator in reducing contact forces and reduces task completion time [5]. When the contact force is reflected via the master actuator to the operator's hand, the teleoperator system is said to be bilateral or force-reflecting.

Two fundamental requirements on bilateral teleoperator systems are stability and transparency. The need for stability is obvious. By "transparency", it is meant that the master should feel to the operator as if the task were being manipulated directly. Appropriate meanings for "transparency" have been pursued in [6]. In general, the requirement has been that the position/force responses of the teleoperator master and slave be identical. Clearly, this definition only applies to those teleoperator systems in which the slaves are controlled to follow the motion of the masters faithfully. In many applications, the position mapping between the master

and slave needs to be scaled either down or up, or rate control needs to be used, especially if the master has a limited workspace. For such situations, transparency is better quantified in terms of the match between the mechanical impedance of the environment encountered by the slave and the mechanical impedance transmitted to or "felt" by the operator at the master [7, 8].

Based on Lawrence's four-channel structure which is only valid for bilateral teleoperation in position-force mode [8], Zhu and Salcudean [1] proposed a general framework for achieving transparency under both position and rate control. The validity of the theory was only verified through simulations.

In this paper, experimental results are presented to verify the theory presented by [1]. It is shown that the proposed scheme possesses good stability and transparency under both position and rate control. Stability is maintained when in contact with both flexible and rigid environments. In Section 2, the theory presented in [1] is summarized briefly. Then in Section 3, the experimental results are demonstrated. It presents *a)* the system set-up, *b)* bilateral teleoperation under position-force control, and *c)* bilateral teleoperation under rate-force control. Motion/force tracking plots and frequency spectra of the hybrid matrices are illustrated. It turns out that in transparent rate mode, unilateral constraints on the slave are reflected as bilateral constraints at the master. A modification to the controller to address this problem is also presented. Finally, Section 4 draws conclusions.

## 2 General Framework for Achieving Transparency under Position and Rate Control

The general framework for achieving transparency under both position and rate control is illustrated in Fig. 1.

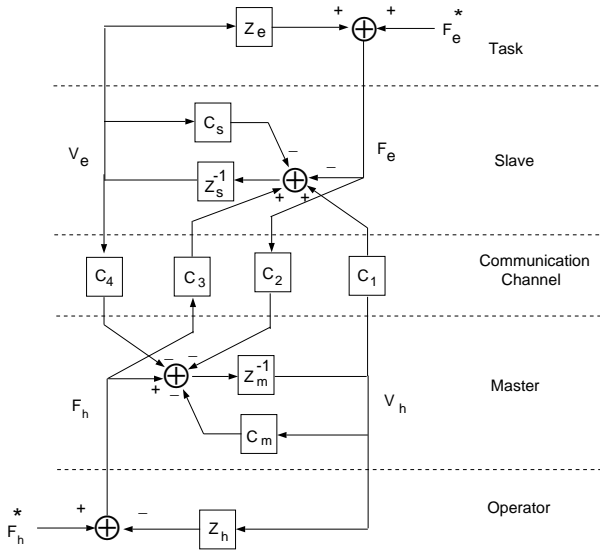


Fig. 1 General teleoperator structure under both position and rate control (from [8])

The blocks in Fig. 1 have the forms as

$$Z_m = M_m s \quad (1)$$

$$C_m = B_m + k_m/s \quad (2)$$

$$Z_s = M_s s \quad (3)$$

$$C_s = B_s + K_s/s \quad (4)$$

$$C_1 = C_s/G \quad (5)$$

$$C_2 = G \quad (6)$$

$$C_3 = 1/G \quad (7)$$

$$C_4 = -C_m G \quad (8)$$

$$Z_h = \text{the impedance of the operator's hand} \quad (9)$$

$$Z_e = \text{the impedance of the environment} \quad (10)$$

where  $M_m$  and  $M_s$  are the masses of the master and the slave respectively,  $C_m$  and  $C_s$  are the transfer functions of the local controllers, and  $F_h^*$  and  $F_e^*$  in Fig. 1 are exogenous forces, hand and environment, respectively.  $G$  is a stable transfer function.

The transmitted impedance felt by the operator, see Fig. 2, can be derived in terms of the block transfer functions as

$$Z_t = \frac{[(Z_m + C_m)(Z_s + C_s) + C_1 C_4] + Z_e(Z_m + C_m + C_1 C_2)}{(Z_s + C_s - C_3 C_4) + Z_e(1 - C_2 C_3)} \quad (11)$$

with the difference between  $Z_t$  and  $Z_e$  being interpreted as a measure of transparency.

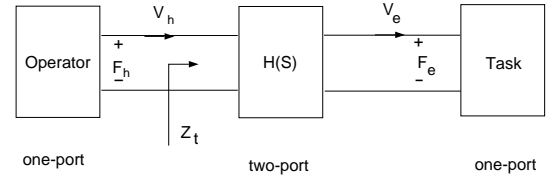


Fig. 2 Network representation of teleoperator system

Under the assumption of identical master and slave subsystems, that is

$$Z_m = Z_s, \quad (12)$$

substituting (5)-(8) into (11) yields

$$Z_t = Z_m + Z_e. \quad (13)$$

The hybrid matrix can be calculated from Fig. 1 and (12) as

$$\begin{bmatrix} F_h \\ -V_e \end{bmatrix} = H(s) \begin{bmatrix} V_h \\ F_e \end{bmatrix} = \begin{bmatrix} Z_m & G \\ -1/G & 0 \end{bmatrix} \begin{bmatrix} V_h \\ F_e \end{bmatrix} \quad (14)$$

It follows that

$$\frac{V_e}{V_h} = \frac{1}{G} \quad (15)$$

We see that the transfer function defines the kinematic correspondence between the master and the slave.

It is clear that transparent position control can be achieved by using

$$G = k \quad (16)$$

where  $k$  is a scale factor. Other types of kinematic correspondence between the master and slave can be realized by setting the proper transfer function  $G$ .

A perfect rate control of a teleoperator system requires that

$$\frac{V_e}{V_h} = \frac{1}{K_v s} \quad (17)$$

where  $K_v$  is a scale factor. Based on the previous results, in order to achieve transparency with perfect rate control, an improper transfer function must be implemented since

$$C_2 = G = K_v s. \quad (18)$$

Instead, a first order filter can be used to achieve rate control with reasonable accuracy, that is

$$G = \frac{K_v s}{1 + T s} \quad (19)$$

where  $T$  is a small time constant which sets the useful velocity tracking frequency range.

*Remark:* Note that the above analysis is based on the assumptions that the master subsystem is exactly the same as the slave subsystem. In order to make  $Z_m =$

$Z_s$ , motion scaling or force scaling is necessary. For example, if  $Z_s/Z_m = \delta \neq 1$ , then either  $V_e$  should be replaced by  $\delta V_e$  or  $F_e$  should be replaced by  $F_e/\delta$  such that  $Z_s/\delta = Z_m$  holds.

### 3 Experimental Results

The experimental set-up is shown in Fig. 3.

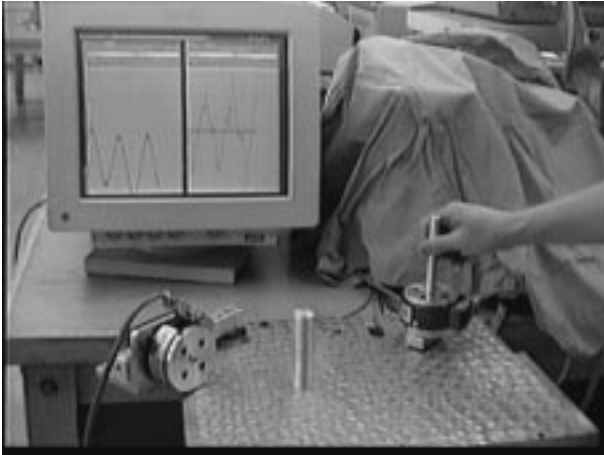


Fig. 3 Experimental set-up

It consists of a one-link master and a one-link slave driven by MAXON Motors RE 035-071 with 4,000 pulse encoders. A planetary gearhead with 10:1 ratio and a harmonic drive with 50:1 ratio are used at the master site and at the slave site, respectively, to increase torques. Each link is equipped with a force sensors UFS 3012A25 U560 by JR<sup>3</sup> Inc.. The distances between the centers of force sensors to the motor driving axes are 65mm for the master and 132mm for the slave, respectively. A handle for the operator is mounted on the force sensor of the master. An aluminum bar of 25mm diameter is fixed to the common base of the master/slave robots to realize a *rigid* contact with the slave. When soft tissues, e.g. human hand, are put between the aluminum bar and the slave, a *flexible* contact is realized. The friction forces reflected at the end-effectors of the master and slave robots are of the order of 0.4N and 6.0N, respectively. The control system is running with a sampling frequency of 500Hz at SPARC 1E VME board by FORCE COMPUTERS Inc. using the VxWorks operating system. The experimental results are illustrated from Fig. 4 to Fig. 17. In these figures, solid lines represent the properties of the master and dashed lines represent the properties of the slave.

In order to make sure  $Z_m = Z_s$ , all the motion/force variables are converted to motor axes. A position means an angle. A velocity means an angular velocity. A force means a torque around the motor axis.

#### A. Position Control

Under position control, the control laws are chosen as

$$G = 0.2 \quad (20)$$

$$C_m = 0.4 + 4.0/s \quad (21)$$

$$C_s = 0.5 + 5.0/s \quad (22)$$

The experimental results are illustrated in Fig. 4 and Fig. 5. Fig. 4 gives position tracking, while Fig. 5 gives force tracking. The systems start with free motion. At about  $t = 4.0s$ , the slave makes contact with a flexible environment until  $t = 8.5s$ . Around  $t = 10.0s$ , the slave contacts an aluminum bar. The results demonstrate very robust performance even in the case of rigid contact. The position/force of the slave are able to track the position/force of the master.

The transfer function of the hybrid matrix defined by

$$\begin{bmatrix} F_h \\ -G \cdot V_e \end{bmatrix} = \begin{bmatrix} h_{11} & h_{12} \\ h_{21} & h_{22} \end{bmatrix} \begin{bmatrix} V_h \\ G \cdot F_e \end{bmatrix} \quad (23)$$

were obtained using MATLAB and are shown from Fig. 6 to Fig. 9. The difference between (23) and (14) is that both  $F_e$  and  $V_e$  are scaled.  $h_{12}$  and  $h_{21}$  are almost around 0db, which reflects perfect transparency.  $h_{11}$  should represent  $Z_m = M_m s$ . The low frequency part indicates that a certain amount of damping exists in the systems, which is resulting from the viscous frictions of the motor drives.  $h_{22}$  represents the transparency error. The high frequency error in  $h_{22}$  is caused by the backlash of the motor drives.

#### B. Rate Control

Under rate control,  $G$  is given by (19) with  $K_v = 0.2$ ,  $T = 0.2$ .  $C_m$  and  $C_s$  are the same as in (21) and (22). The experimental results are illustrated in Fig. 10 and Fig. 11. The systems start with free motion. The slave is in contact with a flexible environment from  $t = 5.5s$  to  $t = 9.5s$ , and contacts the aluminum bar starting at  $t = 11.5s$ , see the dashed line of Fig. 11. In Fig. 10, the solid line denotes the scaled position of the master, while the dashed line denotes the velocity of the slave. Very good tracking is demonstrated. In Fig. 11, the force of the slave (dashed line) is the integral of the force of the master (solid line) during flexible/rigid contact. The center line is the derivative of the dashed line, which is used to compare with the solid line.

The transfer functions of the hybrid matrix defined by (23) are shown from Fig. 12 to Fig. 15.  $h_{12}$  is close to  $s$ , while  $h_{21}$  is close to  $1/s$ .  $h_{11}$  should represent  $Z_m = M_m s$  too. The low frequency part indicates that a certain amount of damping exists in the systems, which results from the viscous frictions of the motor drives.  $h_{22}$  represents the transparency error. The high

frequency error in  $h_{22}$  is caused by the backlash of the motor drives.

Under rate control, where  $G$  is defined by (19), the slave subsystem behaves as an integral of the master subsystem. This causes problems for unilateral constraints as illustrated in Fig. 11. When the slave encounters a flexible/rigid unilateral environment, the teleoperated system exhibits a “sticking” behavior—it is difficult to move against the environment, but also difficult to move away from it. It means that a unilateral constraint at the slave site results in a bilateral constraint at the master site, even though good transparency is achieved according to (13). In order to reflect the unilateral behavior,  $C_3$  in (7) is modified to

$$C_3 = \begin{cases} 0 & F_e \cdot P_h < 0 \ \& \ |P_h - K_v \cdot V_e| \geq \epsilon \\ \frac{1+T_s}{K_v s} & \text{otherwise} \end{cases} \quad (24)$$

where  $P_h$  denotes the master position.  $\epsilon$  is a small positive constant which forms the threshold for the unilateral constraint correction. (24) means that when the constraint opposes the motion, the controller is unchanged, otherwise, the integral force at the slave site is set to zero.

The experimental results are shown in Fig. 16 and Fig. 17. When the master is pulled away from the unilateral constraint,  $F_e$  goes to zero immediately.

## 4 Conclusion

The performance of a teleoperator system can be greatly improved by feeding the operator with the force applied to the slave. With a four-channel transparent architecture, the task impedance can be faithfully reconstructed at the master side to make the system transparent. The kinematic correspondence between the master and slave could be more general than a simple position to position correspondence. As two special cases of position and rate control, the design and analysis presented in the authors’ previous paper are verified in this paper through real-time experiments. The experimental results have demonstrated that the proposed approach possesses very good robustness against uncertainty, while providing transparency under both position and rate control.

## References

- [1] M. Zhu and S. E. Salcudean, “Achieving transparency for teleoperator systems under position and rate control,” *Proc. of IROS’95*, 1995.
- [2] Kazerooni, H., “Human/robot interaction via the transfer of power and information signals: Parts i and ii,” *Proc. of 1989 IEEE Int. Conf. Robot. Automat.*, pp.1632-1649, 1989.
- [3] Hunter, I., Lafontaine, S., Nielsen, P., Hunter, P., and Hollerbach, J., “A microrobot for manipulation and dynamical testing of single living cells,” *Proc. IEEE Micro Electro Mechanical Systems*, pp.102-106, 1989.
- [4] Iwata, H., “Artificial reality with force feedback: Development of desktop virtual space with compact master manipulator” *Computer Graphics*, vol.24, no.4, 1990.
- [5] Stokic, D., Vukobratovic, M., and Hristic, D., “Implementation of force feedback in manipulation robots,” *Int. J. Robotics Research*, vol.5, pp.66-76, 1986.
- [6] Yokokohji, Y., and Yoshikawa, T., “Bilateral control of master-slave manipulators for ideal kinesthetic coupling,” *Proc. 1992 IEEE Int. Conf. Robot. Automat.*, 1992.
- [7] Hannaford, B., “Scaling impedance and power flows in force reflecting teleoperation,” *Robotics Research, ASME*, vol.26, 1990.
- [8] Lawrence, D. A., “Designing teleoperator architecture for transparency,” *Proc. 1992 IEEE Int. Conf. Robot. Automat.*, 1992.

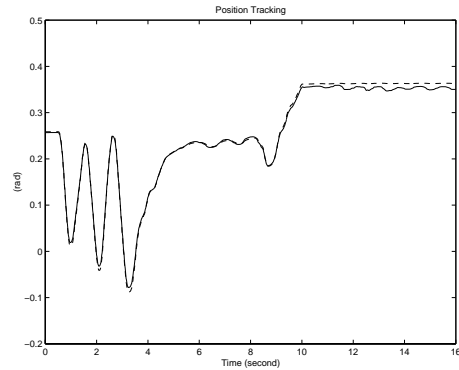


Fig. 4 Position tracking under position control

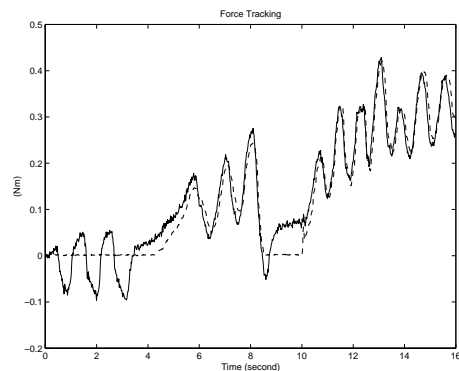


Fig. 5 Force tracking under position control

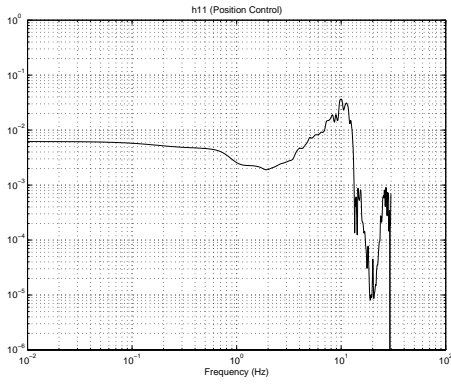


Fig. 6  $h_{11}$  under position control

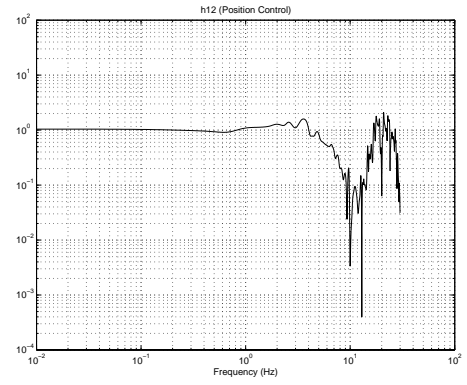


Fig. 7  $h_{12}$  under position control

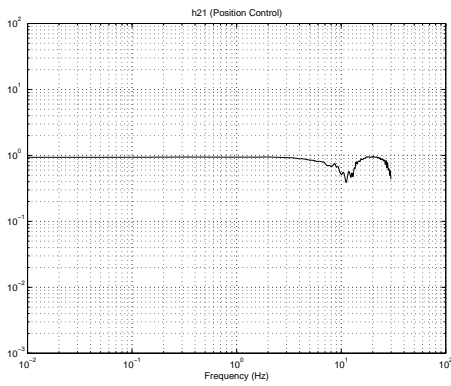


Fig. 8  $h_{21}$  under position control

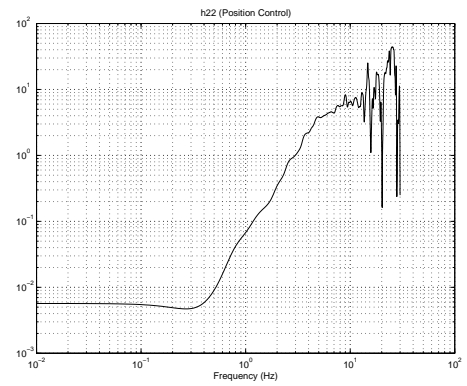


Fig. 9  $h_{22}$  under position control

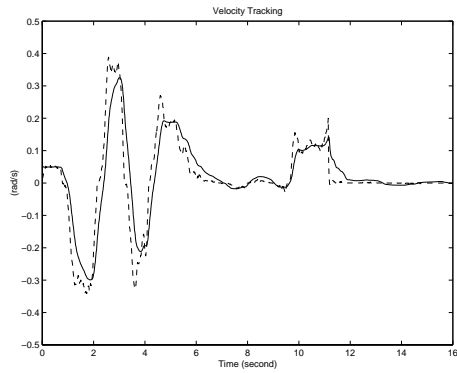


Fig. 10 Velocity tracking under rate control

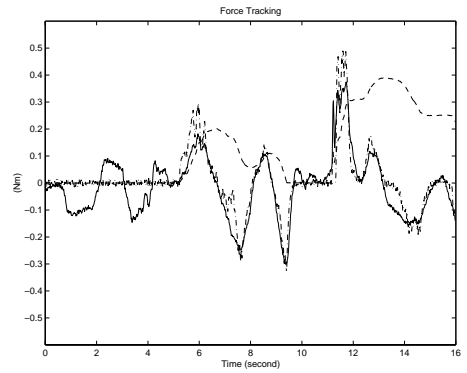


Fig. 11 Force tracking under rate control

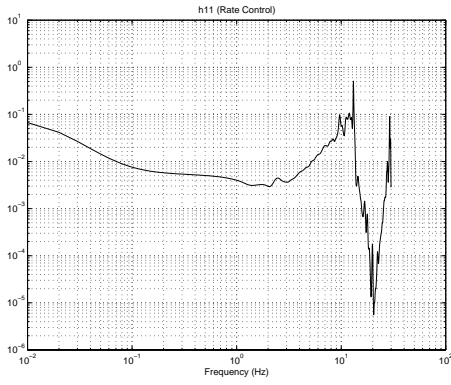


Fig. 12  $h_{11}$  under rate control

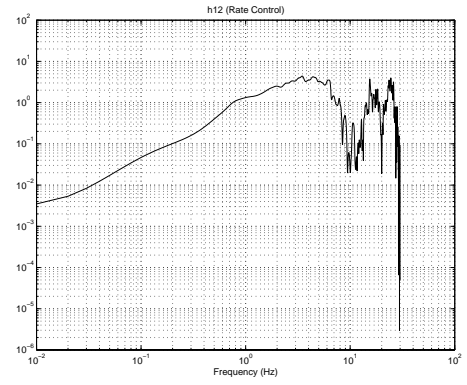


Fig. 13  $h_{12}$  under rate control

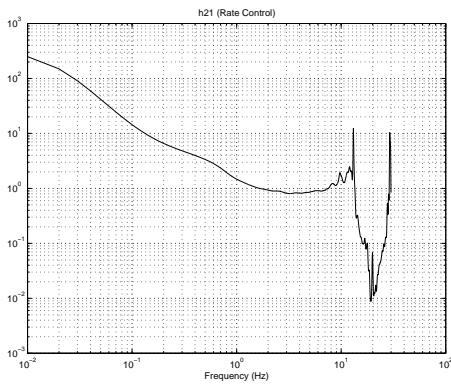


Fig. 14  $h_{21}$  under rate control

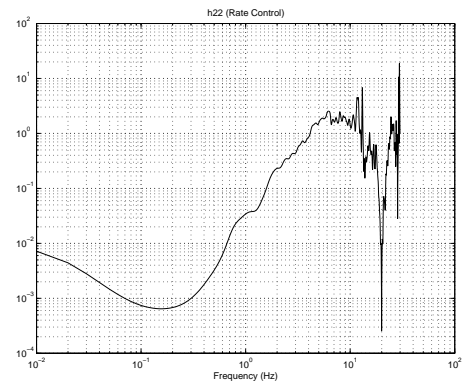


Fig. 15  $h_{22}$  under rate control

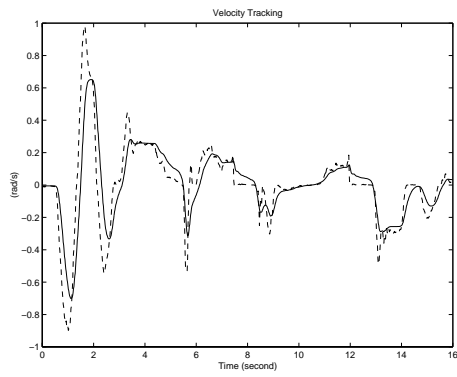


Fig. 16 Velocity tracking under rate control with unilateral constraint correction

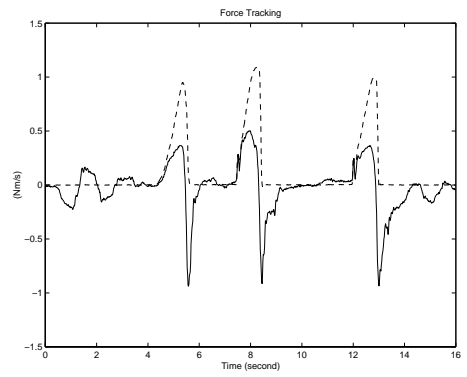


Fig. 17 Force tracking under rate control with unilateral constraint correction